

Analysis of phase error effects in multishot diffusion-prepared turbo spin echo imaging

Anh T. Van¹, Barbara Cervantes², Hendrik Kooijman³, Dimitrios C. Karampinos²

¹Zentralinstitut für Medizintechnik, Technical University of Munich, Garching, Germany; ²Department of Diagnostic and Interventional Radiology, Technical University of Munich, Munich, Germany; ³Philips Healthcare, Hamburg, Germany

Correspondence to: Anh T. Van. Boltzmannstrasse 11, Zentralinstitut für Medizintechnik, Technical University of Munich, Garching 85748, Germany. Email: anh.van@tum.de.

Background: To characterize the effect of phase errors on the magnitude and the phase of the diffusion-weighted (DW) signal acquired with diffusion-prepared turbo spin echo (dprep-TSE) sequences.

Methods: Motion and eddy currents were identified as the main sources of phase errors. An analytical expression for the effect of phase errors on the acquired signal was derived and verified using Bloch simulations, phantom, and *in vivo* experiments.

Results: Simulations and experiments showed that phase errors during the diffusion preparation cause both magnitude and phase modulation on the acquired data. When motion-induced phase error (MiPe) is accounted for (e.g., with motion-compensated diffusion encoding), the signal magnitude modulation due to the leftover eddy-current-induced phase error cannot be eliminated by the conventional phase cycling and sum-of-squares (SOS) method. By employing magnitude stabilizers, the phase-error-induced magnitude modulation, regardless of its cause, was removed but the phase modulation remained. The *in vivo* comparison between pulsed gradient and flow-compensated diffusion preparations showed that MiPe needed to be addressed in multi-shot dprep-TSE acquisitions employing magnitude stabilizers.

Conclusions: A comprehensive analysis of phase errors in dprep-TSE sequences showed that magnitude stabilizers are mandatory in removing the phase error induced magnitude modulation. Additionally, when multi-shot dprep-TSE is employed the inconsistent signal phase modulation across shots has to be resolved before shot-combination is performed.

Keywords: Diffusion-prepared turbo spin echo (dprep-TSE); motion-induced phase errors (MiPe); eddy currents; flow-compensation; body diffusion

Submitted Feb 28, 2017. Accepted for publication Mar 21, 2017.

doi: 10.21037/qims.2017.04.01

View this article at: <http://dx.doi.org/10.21037/qims.2017.04.01>

Introduction

Diffusion-weighted (DW) two-dimensional (2D) single-shot echo planar imaging (SS-EPI) is the most commonly used diffusion imaging technique since it is fast and is not affected by phase variations across different diffusion-encoding periods. However, when moving to applications outside the brain or high isotropic resolution, disadvantages of SS-EPI become more dramatic, leading to the exploration for alternative methods. The disadvantages of SS-EPI include: (I) geometric distortion due to B0

inhomogeneity and eddy currents; (II) long echo time (TE) leading to low signal to noise ratio (SNR) for tissues with short T2; and (III) blurring for tissues with short T2* (1-3).

The disadvantages of SS-EPI originate from its long readout duration and low bandwidth in the phase encoding direction. By segmenting the readout into multiple interleaved shots, the readout duration reduces while the bandwidth in the phase encoding direction increases, resulting in less geometric distortion and T2* blurring (4-6). Due to shot-to-shot phase inconsistency induced by motion

during the diffusion encoding, multi-shot DW techniques require an accompanied phase correction method (7-12).

DW turbo spin echo (DW-TSE) techniques also offer the capability to alleviate the disadvantages of SS-EPI by employing radio frequency (RF) refocusing pulses between each k-space line or small groups of k-space lines (13-16). Even when performed in a single-shot mode, TSE-based techniques have to deal with the motion-induced phase error (MiPe) due to the additional violation of the Carr-Purcell-Meiboom-Gill (CPMG) condition (16-20).

Diffusion-weighting driven-equilibrium (DW-DE) techniques have been already long ago investigated as alternatives to DW SS-EPI due to the prevailing hardware limitations of early MR systems and the need to reduce off-resonance-induced distortions (21,22). Recently, DW-DE techniques are regaining their popularity due to the increasing demand for high isotropic resolution diffusion imaging primarily in body applications (23-33). DW-DE can be flexibly combined with any type of readout schemes, enabling optimization for resolution, distortion, and SNR. Successful studies of DW-DE in combination with turbo fast low angle shot (turboFLASH), stimulated echo acquisition mode (STEAM), TSE, single-shot stimulated echo planar imaging (ss-STEPI), and balanced steady state free precession (bSSFP) have been reported in the brain, in peripheral nerves, in the heart, and in the carotid vessel wall (21-23,25-34). However, to the best of our knowledge, there has been no study on analyzing and characterizing the effect of phase errors during the diffusion encoding to the signal acquired with DW-DE techniques. Instead, it has been only briefly reported that phase errors during the diffusion encoding leads to signal magnitude modulation (22,23,27). Furthermore, without clear explanation, most of the DW-DE studies employed a single-shot acquisition approach unless a motion-compensated diffusion-encoding scheme was used. Therefore, the optimization of DW-DE acquisitions requires a comprehensive characterization of the sensitivity of DW-DE techniques to the phase error effects.

The aim of the present study is to characterize the effect of phase errors on the magnitude and the phase of the DW signal acquired with DW-DE TSE sequences, which in recent literature have been labeled as diffusion-prepared TSE sequences (dprep-TSE). The TSE readout scheme is chosen since it is less sensitive to contamination with non-DW magnetization caused by T1 relaxation during the readout and has a simpler signal evolution that better preserves the prepared diffusion contrast. The sources of

phase error in consideration in the subsequent analysis include motion and eddy current effects.

Theory

Sources of phase errors in dprep-TSE sequences

MiPe

Diffusion imaging contrast is achieved by employing magnetic field gradients to encode the random motion of spins. Besides the desired random motion of spins, the employed diffusion gradients are also sensitive to any other types of motion experienced by the object being imaged. These undesired types of motion include but are not limited to scanner vibration, voluntary and involuntary object movements, cardiac pulsation, and respiration. When an object moves in the presence of a magnetic field gradient, the transverse magnetization component of its spins accumulates phase. In most cases, the undesired motion is spatially smooth and the accumulated phase is uniform for all spins within an image voxel. As a result, the DW signal of a moving voxel is contaminated with an additional phase, called MiPe, as compared to the case when the voxel is stationary. Previous studies have shown that rigid-body translation and rotation leads to a spatially linear MiPe across the object while non-rigid-body motion gives rise to spatially higher-order components (7,12).

Eddy-current-induced phase error

Eddy currents are a common problem in diffusion imaging due to the necessity of switching on and off gradients with maximum amplitude at maximum slew rate. Eddy currents distort the designed diffusion gradients and lead to incomplete refocusing after diffusion encoding. This leftover gradient field induces undesirable phase accumulation, called eddy-current-induced phase error, even on stationary spins. Eddy-current-induced phase error varies spatially. However, unlike MiPe, which may change from repetition to repetition of the acquisition, eddy-current-induced phase error will be the same for each repetition if the applied diffusion gradient is the same.

Effects of phase error in dprep-TSE sequences

In diffusion prepared sequences, at the end of the diffusion-encoding period, transverse magnetization is stored back to the longitudinal direction with a 90° tip-up (echo-reset) RF pulse and the remaining transverse magnetization after

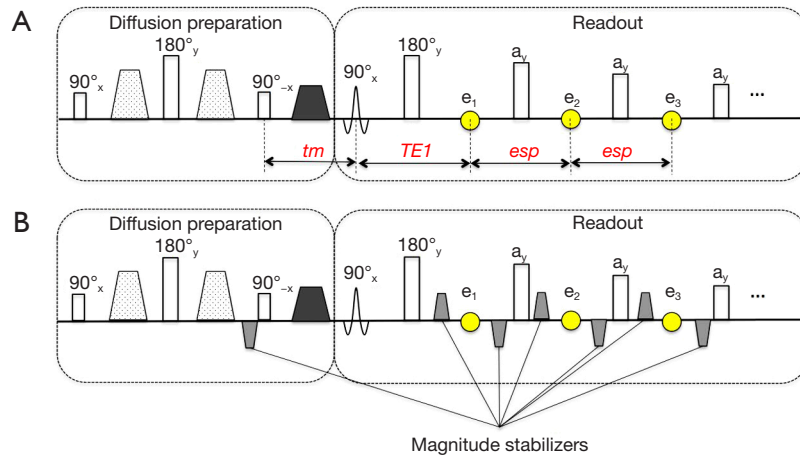


Figure 1 Diffusion-prepared turbo-spin echo sequence (A) without magnitude stabilizers and (B) with magnitude stabilizers.

tip-up is crushed (Figure 1A). The prepared longitudinal magnetization is then ready to be used for image formation with any type of readout (TSE in the context of the present study). Without loss of generality, considering the diffusion preparation as shown in Figure 1A, the magnetization of a voxel at the end of the diffusion preparation, before the tip-up RF pulse is

$$M_{xy}(90_{-x}^-) = M_{prep} e^{jn/2} e^{j\phi_{voxel}} \quad [1]$$

M_{prep} is the magnitude of the prepared magnetization, which is subject to T2-decay and diffusion attenuation. The combination of excitation along the x-axis and refocusing along the y-axis results in a magnetization at the spin echo along the y-axis and the $\pi/2$ phase term. The ϕ_{voxel} phase term comes from the phase error after the diffusion-encoding period and is assumed to be uniform across the voxel. Applying the tip-up RF pulse to the magnetization in Eq. [1] results in the prepared longitudinal magnetization

$$M_z(90_{-x}^+) = M_{prep} \cos \phi_{voxel} \quad [2]$$

Taking into account T1-relaxation between the tip-up RF pulse and the excitation pulse of the TSE readout module, the longitudinal magnetization right before TSE readout excitation is

$$M_z(90_{+x}^-) = M_{prep} \cos \phi_{voxel} e^{-tm/T1} + M_0(1 - e^{-tm/T1}) \quad [3]$$

where M_0 is the equilibrium magnetization of the voxel, and tm is the time between the tip-up pulse and the TSE

$$M_{xy}^k = a_k e^{jn/2} M_{prep} \cos \phi_{voxel} e^{-tm/T1} = \begin{cases} a_k M_{prep} e^{-tm/T1} |\cos \phi_{voxel}| e^{jn/2}, & -\frac{\pi}{2} < \phi_{voxel} < \frac{\pi}{2} \\ a_k M_{prep} e^{-tm/T1} |\cos \phi_{voxel}| e^{j3\pi/2}, & \text{otherwise} \end{cases} \quad [7]$$

readout excitation pulse. The transverse magnetization at the first echo (marked with e_1 in Figure 1A) with echo time $TE1$ is

$$M_{xy}^1 = e^{-TE1/T2} \left[M_{prep} \cos \phi_{voxel} e^{-tm/T1} + M_0(1 - e^{-tm/T1}) \right] e^{jn/2} \quad [4]$$

When all the refocusing pulses in the TSE readout are perfect 180° pulses, the transverse magnetization at the k^{th} echo with echo spacing of esp is

$$M_{xy}^k = e^{-(TE1+(k-1)esp)/T2} \left[M_{prep} \cos \phi_{voxel} e^{-tm/T1} + M_0(1 - e^{-tm/T1}) \right] e^{jn/2} \quad [5]$$

Thanks to the tip-up RF pulse, the Meiboom-Gill (MG) condition for a stable steady-state echo train is satisfied regardless of the phase error induced during the diffusion-encoding period. Therefore, even when the TSE refocusing pulses are $<180^\circ$, the transverse magnetization at the k^{th} echo can be expressed as

$$M_{xy}^k = a_k \left[M_{prep} \cos \phi_{voxel} e^{-tm/T1} + M_0(1 - e^{-tm/T1}) \right] e^{jn/2} \quad [6]$$

where a_k represents the signal decay at the k^{th} echo and is dependent on the flip angles of the echo train, T1, and T2. Except for few initial echoes, in most cases a_k represents a slower decay than the pure T2-decay.

Eq. [6] shows that the echo signal is a function of the phase error, ϕ_{voxel} . When $tm \ll T1$ and the magnitude of the prepared magnetization M_{prep} is significant (e.g., low b-value diffusion encoding), $M_{prep} e^{-tm/T1} \cos \phi_{voxel} \gg M_0(1 - e^{-tm/T1})$ and Eq. [6] can be rewritten as

Eq. [7] implies that in the presence of a uniform MiPe ϕ_{voxel} across the voxel and negligible T1 effect during the time tm , the voxel signal magnitude is modulated by $|\cos\phi_{voxel}|$ and the voxel signal phase toggles between $\pi/2$ and $3\pi/2$ states.

At this point we have shown analytically that phase errors at the end of the diffusion-encoding period cause both magnitude and phase modulation of the acquired signal. The phase-error-dependent magnitude modulation is irreversible and can corrupt DW images and derived quantitative diffusion parameters regardless of whether the data acquisition is single-shot or multi-shot. The phase toggling, however, only affects the DW images when a multi-shot acquisition is employed.

Mitigation of phase error effects

Phase cycling and sum-of-squares (SOS)

When the same phase error is repeated from acquisition to acquisition, a previous study proposed to first perform two acquisitions that have phases of tip-up RF pulses 90° from each other and to then take the SOS of the two acquisitions to mitigate the echo signal dependence on phase errors (22). This phase cycling and SOS method was established based on the signal evolution in Eq. [7]. The analytical result obtained in Eq. [7] is achieved with the tip-up RF pulse along the $-x$ axis. When the tip-up RF pulse is along the $-y$ axis, Eq. [7] becomes

$$M_{xy}^k = a_k e^{j\pi/2} M_{prep} e^{-tm/T1} \cos\left(\phi_{voxel} - \frac{\pi}{2}\right);$$

$$= a_k e^{j\pi/2} M_{prep} e^{-tm/T1} \sin\phi_{voxel}$$
[8]

Taking the square root of the SOS of Eqs. [7] and [8], we have

$$|M_{xy}^{k,sos}| = a_k M_{prep} e^{-tm/T1}$$
[9]

which is independent of the phase error.

However, it is important to point out that Eqs. [7] and [8] hold true only when $tm \ll T1$ and the prepared magnetization M_{prep} has significantly high amplitude. When moderate to high b-value diffusion encoding is applied in tissues with moderate T1 and high diffusivity, the signal evolution follows Eq. [6]. In this case, it can be shown that the combination of the phase cycling and

$$M_{xy}^1 = \frac{e^{j\pi/2}}{N_{spin}} \left[M_0 (1 - e^{-tm/T1}) \sum_{i \in voxel} e^{j\theta_i} + M_{prep} e^{-tm/T1} \sum_{i \in voxel} \cos(\phi_{voxel} - \theta_i) e^{j\theta_i} \right] e^{-TE1/T2}$$
[13]

the SOS method results in a signal that still depends on the phase error, and has the following functional form:

$$|M_{xy}^{k,sos}| = f(\cos\phi_{voxel} + \sin\phi_{voxel})$$

Magnitude stabilizers

Another later proposed method for mitigating the phase-error-dependent signal modulation applied dephasing gradients before the tip-up RF pulse and a rephasing/dephasing gradient pairs (labeled as magnitude stabilizers in *Figure 1B*) around the echoes (23,26). The heuristic reason for this approach was to exploit the dephasing effect of the gradient before the tip-up RF pulse to create a uniform phase distribution over the voxel, at the cost of 50% of the signal, regardless of the signal phase. The rephasing gradient was added later in the readout module to form an echo. Besides demonstrating that the proposed method indeed resulted in high quality artifact-free DW images and diffusion maps in single-shot acquisition mode, there exists no analytical characterization of the performance of the method in the presence of phase errors.

In analogy to Eq. [1] and taking into account the magnitude stabilizer effect, the magnetization of a voxel at the end of the diffusion preparation, after the first magnitude stabilizer pulse and before the tip-up RF pulse is

$$M_{xy}(90_{-x} -) = M_{prep} e^{j\pi/2} e^{j\phi_{voxel}} \frac{1}{N_{spin}} \sum_{i \in voxel} e^{-j\theta_i}$$
[10]

where θ_i is the phase introduced by the magnitude stabilizer gradient on the i^{th} spin of the voxel, N_{spin} is the total number of spins in the voxel. Trivially, the longitudinal magnetization after the tip-up pulse and before the TSE readout excitation pulse, respectively, are

$$M_z(90_{-x} +) = M_{prep} \frac{1}{N_{spin}} \sum_{i \in voxel} \cos(\phi_{voxel} - \theta_i)$$
[11]

$$M_z(90_{+x} -) = M_0 (1 - e^{-tm/T1})$$

$$+ M_{prep} e^{-tm/T1} \frac{1}{N_{spin}} \sum_{i \in voxel} \cos(\phi_{voxel} - \theta_i)$$
[12]

With the refocusing lobe of the magnitude stabilizer in consideration, the transverse magnetization at the first echo (marked with e_1 in *Figure 1B*) with echo time $TE1$ is

Since the magnitude stabilizers are designed to introduce a complete dephasing of the signal within a voxel, i.e., $\sum_{i \in \text{voxel}} e^{j\theta_i} = 0$, Eq. [13] can be reduced to

$$M_{xy}^1 = \frac{1}{2} M_{prep} e^{-tm/T1} e^{-TE1/T2} e^{j(\phi_{\text{voxel}} + \pi/2)} \quad [14]$$

The presence of a magnitude stabilizer lobe after the first echo of the TSE readout with a sign opposite to the sign of the lobe preceding the first echo of the TSE readout undoes the “rephasing effect” in Eq. [13] resulting in a dephased transverse magnetization. This dephased magnetization is later refocused by the second refocusing pulse of the TSE readout and the next refocusing lobe of the magnitude stabilizer to form the second echo. In this manner, all the later echoes are formed and the transverse magnetization at the k^{th} echo of the TSE readout with echo spacing of esp is

$$M_{xy}^k = \frac{1}{2} M_{prep} e^{-tm/T1} e^{-[TE1+(k-1)esp]/T2} e^{j(\phi_{\text{voxel}} + \pi/2)} \quad [15]$$

when all the refocusing pulses are 180° . When the refocusing pulses are not 180° , similar to Eq. [6], the transverse magnetization at the k^{th} echo becomes

$$M_{xy}^k = a_k \left[\frac{1}{2} M_{prep} e^{-tm/T1} e^{-[TE1+(k-1)esp]/T2} e^{j(\phi_{\text{voxel}} + \pi/2)} \right] \quad [16]$$

With proper design of the echo train, except for several initial echoes, a_k is a real positive parameter representing a slower decay than the pure T2-decay.

Eq. [16] indicates that with the application of magnitude stabilizers and under the assumption of voxel-wise uniform MiPe, the voxel signal magnitude is independent of the phase error while the phase varies linearly with the phase error.

Therefore, a dprep-TSE sequence employing magnitude stabilizers becomes very similar to the conventional spin echo EPI DW sequence in terms of how phase errors affect the measured signal. If the acquisition is single-shot, the phase-error-induced signal phase modulation can be ignored. When a multi-shot acquisition is needed, such as in the case of high-resolution three-dimensional (3D) diffusion imaging, if the phase error is constant across shots (e.g., eddy-current-induced phase errors) the phase-error dependence can also be ignored. However, with multi-shot imaging in the presence of a time-varying phase error (e.g., MiPe) the signal phase modulation has to be accounted for before the shots are combined (8,9,11,12).

When comparing Eqs. [6] and [16], it is important to notice that magnitude stabilizers remove not only the

phase-error-induced magnitude modulation but also the dependency of the echo signal on the unprepared T1-recoverd signal regardless of the T1 value of the tissue being imaged and the duration of the time tm . This additional benefit of the magnitude stabilizers has been previously reported in a T2-prepared sequence with fast gradient echo readout (35). What remains is just a decay of the prepared signal due to T1-relaxation during the interval tm .

It is important to notice that the results obtained in Eq. [6] and [16] are under the assumption that the motion-induced phase after the diffusion preparation is uniform across the voxel. When the uniform phase assumption is not valid, which is the case in the presence of intra-voxel dephasing, the phase-error-dependent magnitude modulation cannot be eliminated even with magnitude stabilizers.

Methods

Bloch simulation

A Bloch simulation was used to illustrate effects of phase errors on the diffusion prepared signal. Uniform phase errors were added to all spins within the simulated voxel before the tip-up RF pulse. The simulated 2D voxel contained 10,000 spins with off-resonance uniformly distributed in -20 – 20 Hz. T2 and T1 relaxation parameters for the voxel were 75 and 1,000 ms, respectively. The diffusion preparation module was composed of $90_x^\circ - 180_y^\circ - 90_x^\circ$ with a preparation TE of 60 ms. The time tm between the tip-up RF pulse and the excitation pulse of the TSE readout was 11 ms. For the TSE readout, a previously optimized flip angle train was used with a TSE factor of 60 and echo spacing of 3.2 ms (34). More specifically, given a certain T1, T2, echo train length, number of start-up echoes, and maximum flip angles, an optimization procedure selected a flip angle train so that the signal approached a certain intensity level after the start up echoes and remained at that level for a designed number of echoes, called the signal plateau length (36). The signal plateau length and later flip angles were chosen to balance the needs for adequate signal and tolerable blurring.

MR measurement

All phantom and *in vivo* experiments were performed on a 3T Philips system (Philips Ingenia, Best, the Netherlands). A multi-shot 3D Cartesian trajectory was used for spatial

encoding.

Phantom experiments were designed to isolate the phase error effects due to eddy currents from those due to motion. The diffusion preparation module used a 90° hard pulse for excitation followed by two adiabatic hyperbolic secant refocusing pulses and ended with a 90° hard pulse for tip-up. Four lobes of diffusion encoding gradients were used straddling the two adiabatic refocusing pulses with pairwise opposite polarities. Two phantom experiments were performed.

In the first phantom experiment, varying phase errors at the end of the diffusion encoding period were added by cycling the phase of the tip-up RF pulse from $-\pi$ to π at $\pi/18$ intervals. The magnitude modulation of the signals obtained without diffusion encoding ($b = 0 \text{ s/mm}^2$) and with diffusion encoding ($b = 600 \text{ s/mm}^2$) along the [1 1 1] direction were investigated.

The second phantom experiment was performed with a b value of 600 s/mm^2 at ten non-collinear directions. This second phantom experiment was designed to visualize eddy current effects and to evaluate the effectiveness of the phase cycling and SOS method in removing the phase-error-induced magnitude modulation. To enable the phase cycling and SOS method, two repetitions with tip-up RF pulse along $-x$ and $-y$ directions were acquired.

For free induction decay (FID) signal cancellation, two phase cycles of the TSE excitation pulses (along $-x$ and x) were acquired and the complex sum of the resulted signals was performed. Other imaging parameters for both phantom experiments were as follows: voxel size = $2.5 \times 2.5 \times 5 \text{ mm}^3$, field of view (FOV) = $120 \times 120 \times 60 \text{ mm}^3$, TE/TR = $60/1,700 \text{ ms}$, TSE factor = 60, SENSE reduction factor = 1.5 A-P and 1.5 S-I, center-out k-space ordering. A 16-channel knee coil was used for both transmitting and receiving the signal.

Skeletal muscle was chosen to showcase the effect of phase errors in *in vivo* data acquired with the dprep-TSE sequence. Four versions of the sequence were used including pulsed gradient diffusion preparation without magnitude stabilizers (PG), pulsed gradient diffusion preparation with magnitude stabilizers (PG-ms), flow-compensated diffusion preparation without magnitude stabilizers (FC), and flow-compensated diffusion preparation with magnitude stabilizers (FC-ms). The flow-compensated diffusion preparation was introduced in the *in vivo* experiment for comparison with the pulsed field gradient diffusion preparation to highlight the time varying nature of MiPe and its effect on the multi-shot dprep-TSE

sequence.

The diffusion preparation module used a 90° hard pulse for excitation followed by two adiabatic hyperbolic secant refocusing pulses and ended with a 90° hard pulse for tip-up. Four lobes of diffusion encoding gradients were used straddling the two adiabatic refocusing pulses with pairwise opposite polarities in the case of pulsed gradient diffusion encoding and with all the same polarities in the case of flow-compensated diffusion encoding (25). Diffusion encoding was applied with a b value of 400 s/mm^2 at seven non-collinear directions. Fat saturation was performed using spectral attenuated inversion recovery (SPAIR) technique with an inversion time of 200 ms. For FID signal cancellation, two phase cycles of the TSE excitation pulses (along $-x$ and x) were acquired and the complex sum of the resulted signals was performed. Other imaging parameters for this *in vivo* data set were as follows: voxel size = $1.5 \times 1.5 \times 6 \text{ mm}^3$, FOV = $145 \times 133 \times 78 \text{ mm}^3$, TE/TR = $60/1,700 \text{ ms}$, TSE factor = 60, SENSE reduction factor = 1.5 A-P and 1.5 S-I, center-out k-space ordering. A 16-channel knee coil was used for both transmitting and receiving the signal.

Results

Bloch simulation results

Figure 2 displays the Bloch-simulated magnitude and phase of the first echo in the TSE readout with respect to the applied phase error. When magnitude stabilizers are not used, the magnitude of the signal exhibits a $|\alpha \cos(\phi_{\text{voxel}} + \beta)|$ modulation (Figure 2A) while the phase toggles between $-\pi/2$ and $\pi/2$ (Figure 2B). Applying the simulation parameters to Eq. [4], we obtained

$$\frac{\beta}{\alpha} = \frac{1 - \exp(-tm/T1)}{\exp(-tm/T1) \exp(-TE_{\text{prep}}/T2)} = 0.028, \text{ meaning that the}$$

unprepared T1-recovered signal is 2.8% of the prepared signal. As it can be seen from Figure 2A,B, the analytical result fits well with the simulation result. With the simulated T1 and T2 of 1,000 and 70 ms, respectively, the effect of T1-relaxation as described in Eq. [6] can be observed in Figure 2A. Notice that the unprepared T1-recovered signal over the time interval tm {the second term in Eq. [6]} is always positive. Therefore, when $|\phi_{\text{voxel}}| > \pi/2$, the z-component of the prepared magnetization {the first term in Eq. [6]} will be negative, leading to a smaller signal amplitude as in the case of $|\phi_{\text{voxel}}| < \pi/2$, where the z-component of the magnetization is positive after the

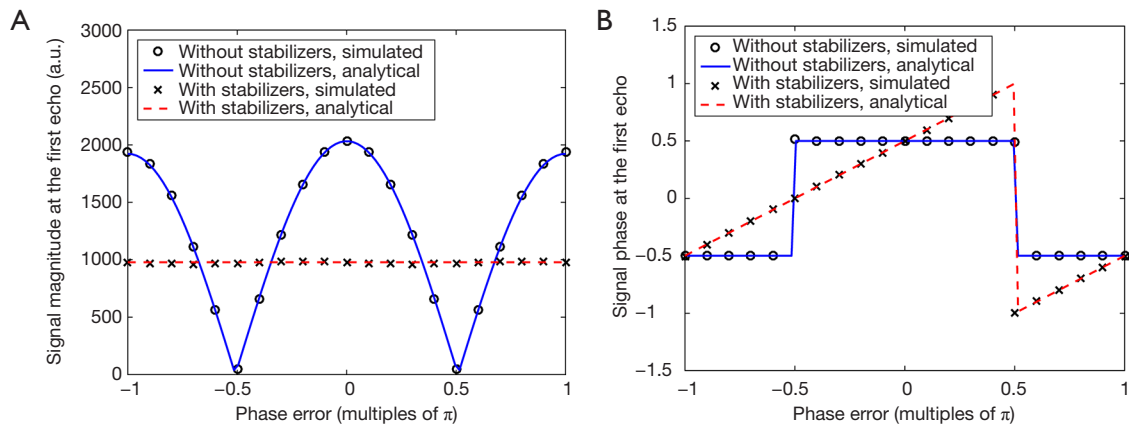


Figure 2 Bloch simulation result of the first echo in TSE readout without and with magnitude stabilizers: (A) echo magnitude; (B) echo phase. Without magnitude stabilizers, the signal magnitude exhibits approximately $|\cos\phi_{voxel}|$ modulation while the signal phase has two discrete states of $-\pi/2$ and $\pi/2$. T1 effect can be observed through the reduced amplitude of the signal at $\phi_{voxel}=\pm\pi$ as compared to the signal at $\phi_{voxel}=0$. With magnitude stabilizers, the dependency of signal magnitude on phase error is removed but the signal phase varies linearly with phase error.

preparation.

Magnitude stabilizers flatten out the magnitude modulation at a cost of 50% loss of the signal (*Figure 2A*) but leave the phase varying linearly with the simulated phase error (*Figure 2B*). The same effect of magnitude stabilizers was expressed analytically in Eq. [16].

Regardless of the applied phase error, the TSE echo train signal obtained with magnitude stabilizers remains stable and exhibits the decay as designed by the flip angle train, meaning after the first few echoes, the signal stays flat for more than 15 echoes and then experiences sub-T2 decay (*Figure 3A*). When magnitude stabilizers are not used, echo train signal varies strongly depending on the applied phase error (*Figure 3B*).

Phantom results

The average image magnitude within two regions of interest (ROIs) in the water phantom is shown with respect to the phase of the tip-up RF pulse in *Figure 4*. Similar to results obtained analytically and through simulation, when diffusion weighting and magnitude stabilizers are not used, the signal magnitude in the ROIs oscillates with $|\alpha_w \cos\phi_{tip-up} + \beta_w|$ (*Figure 4A*). Regarding the T1-relaxation effect, the unprepared T1-recovered signal is 4.6% and 5.4% of the prepared signal in ROI 1 and ROI 2, respectively.

When diffusion weighting is applied, spatially varying

phase errors induced by eddy currents shift the magnitude curve of ROI 1 by 0.21π and that of ROI 2 by 0.14π (*Figure 4B*). In comparison with the signal behavior at $b=0$ described above, diffusion encoding attenuates the prepared magnetization while the unprepared T1-recovered signal remains unchanged. Therefore, the T1-relaxation effect is worse at $b=600 \text{ s/mm}^2$. More specifically, the unprepared signal is 17.6% and 21.1% of the prepared signal in ROI 1 and ROI 2, respectively. When magnitude stabilizers are used, even with diffusion weighting, the signal magnitude within the ROI is independent of the phase of the tip-up RF pulse at a cost of 50% signal loss (*Figure 4C*).

Figure 5A shows the average signal magnitudes within an ROI in the water phantom across ten diffusion encoding directions when the tip-up RF pulse is along $-x$, along $-y$, and the SOS of the two. Due to eddy-current-induced phase errors, the “tip-up $-x$ ” and “tip-up $-y$ ” curves exhibit the expected opposite signal variation. The “SOS” curve still shows significant oscillation across diffusion directions, implying the inadequate performance of the phase cycling and SOS method in resolving the eddy-current-induced magnitude modulation. The same behavior of the “SOS” curve is also observed in other locations in the water phantom (*Figure 5B*). Magnitude stabilizers give more stable signal across different diffusion encoding directions (*Figure 5C*). When the phase cycling and SOS method is used, the instability of DW magnitude leads to the fluctuation in the estimated apparent diffusion coefficient

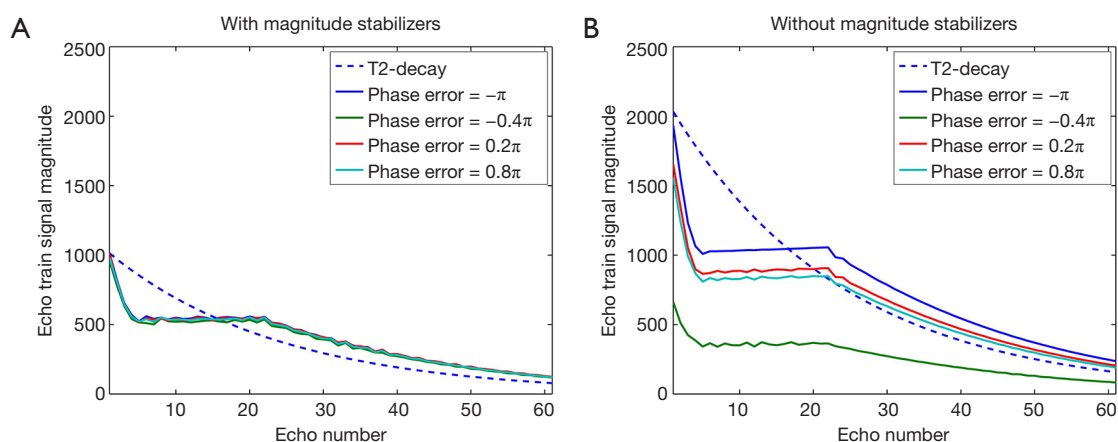


Figure 3 Bloch simulation result of TSE readout echo train with (A) and without (B) magnitude stabilizers. Solid lines correspond to echo train signal with different applied phase errors. Dash lines correspond to the T2 decay. Without magnitude stabilizers, the echo train magnitude varies with the phase error. With magnitude stabilizers, the echo train magnitude is independent of the phase error and experiences a sub-T2 decay.

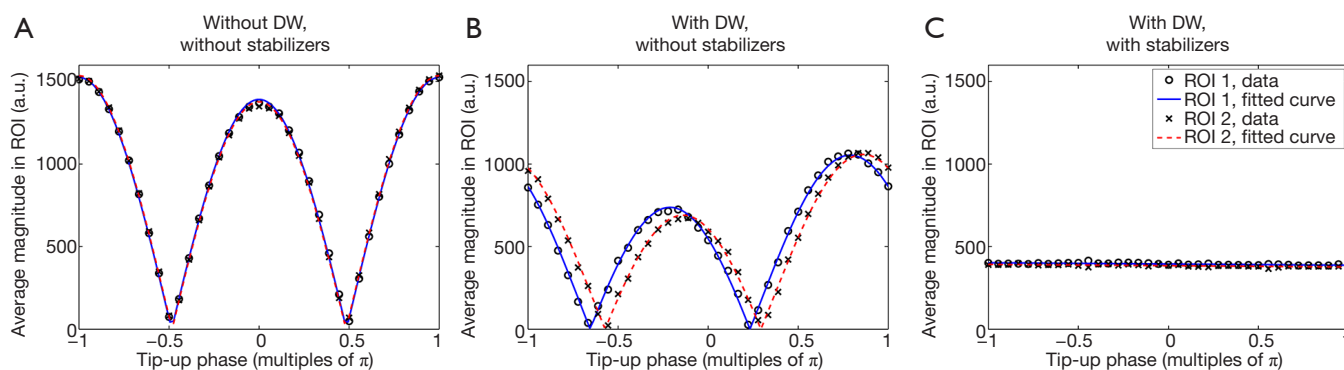


Figure 4 The image magnitude modulation as a function of the tip-up RF pulse phase on the water phantom. Without diffusion encoding and without magnitude stabilizers (A), average signal magnitudes of two ROIs exhibit approximately $|\cos\phi_{tip-up}|$ modulation. When diffusion encoding is added (B), both curves are shifted due to the presence of eddy-current-induced phase error. More severe T1 effect can be observed since diffusion encoding attenuates the prepared magnetization. Magnitude stabilizers remove the dependency of signal magnitude on tip-up phase, and eddy-current-induced phase error (C).

(ADC) per direction (Figure 6A) and an erroneously high FA (Figure 6B). Instead, magnitude stabilizers result in lower variation in estimated ADC per direction (Figure 6C) and low FA values (<0.05 , Figure 6D).

In vivo results

DW images of the calf muscle obtained with four variations of the dprep-TSE sequence are shown in Figure 7A-D. The corresponding ADC maps are shown in Figure 7E-H. When magnitude stabilizers are not used (Figure 7A,B), magnitude modulation can be observed in the muscle area

and fat signal appears hyper-intensive as if no fat saturation was done. When magnitude stabilizers are used but the diffusion preparation is not flow-compensated, signal loss is apparent due to the motion-induced phase inconsistency between different shots (Figure 7C). Magnitude stabilizers and flow-compensated diffusion preparation enable clean DW images and reasonable ADC values of $1.69 \times 10^{-3} \text{ mm}^2/\text{s}$.

Discussion

The dprep-TSE sequence is a candidate for distortion-mitigated DW imaging in applications with high B0

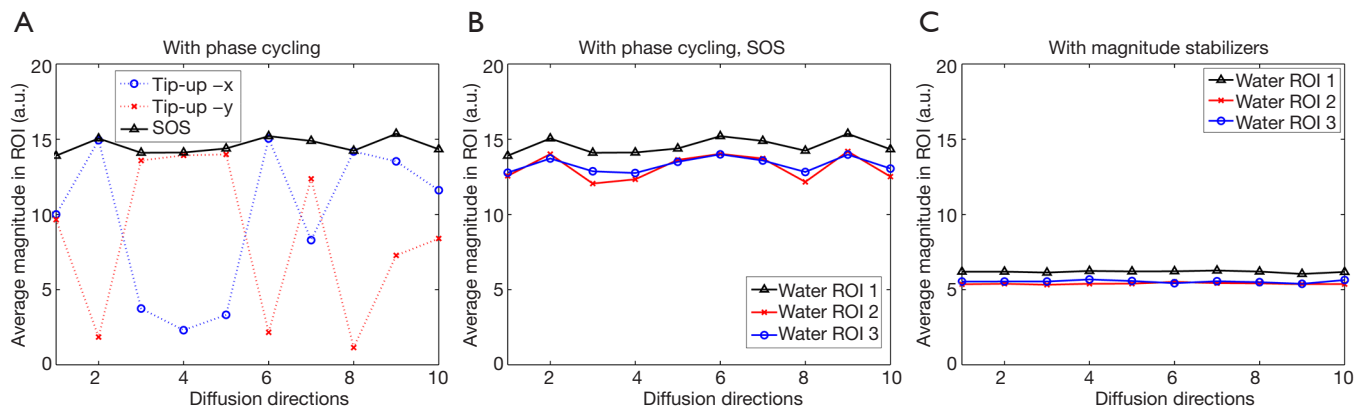


Figure 5 (A) Average diffusion-weighted signal across diffusion directions in a single water ROI with two phase cycles and SOS, (B-C) average diffusion-weighted signal across diffusion directions in three water ROIs with phase cycling (B) and with magnitude stabilizers (C). The “tip-up -x” and “tip-up -y” curves show the expected opposite evolution with respect to the diffusion encoding direction (A). SOS of the two curves still shows dependency on the diffusion encoding direction (B) while acquisition with magnitude stabilizers does not (C).

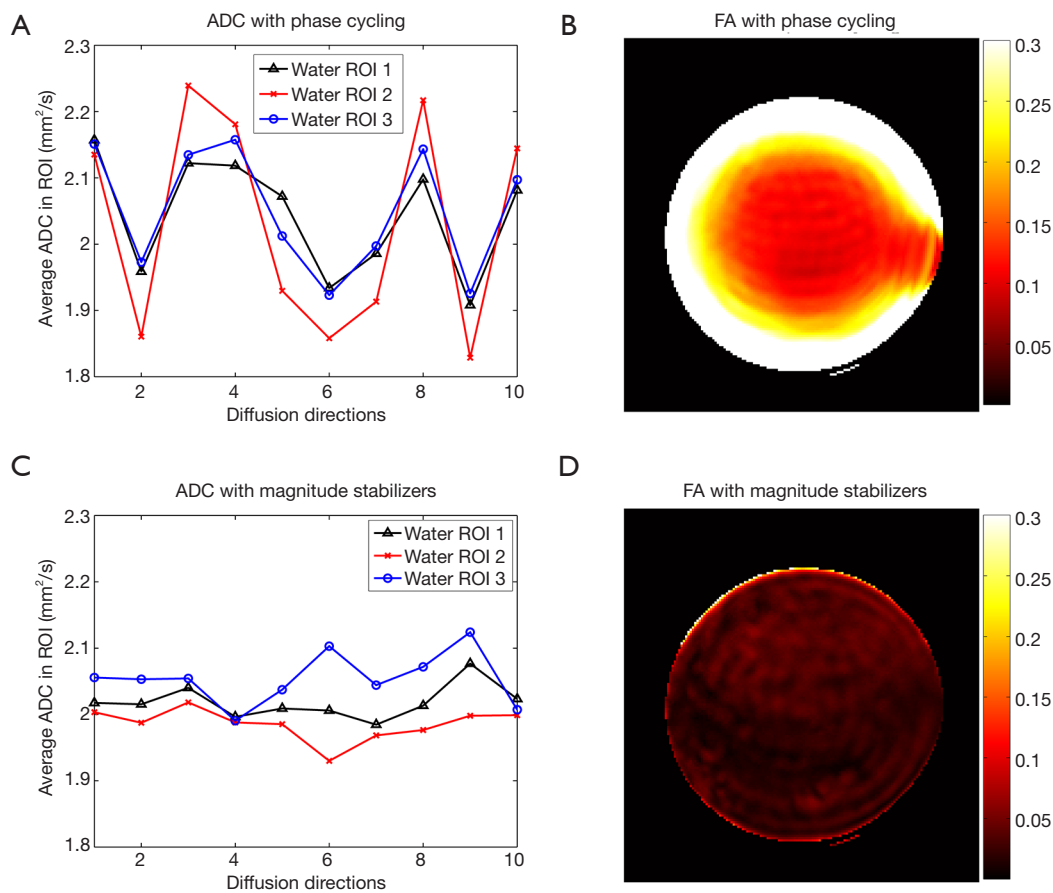


Figure 6 Estimated phantom ADC per direction in 3 ROIs and FA maps with phase cycling (A,B) and with magnitude stabilizers (C,D).

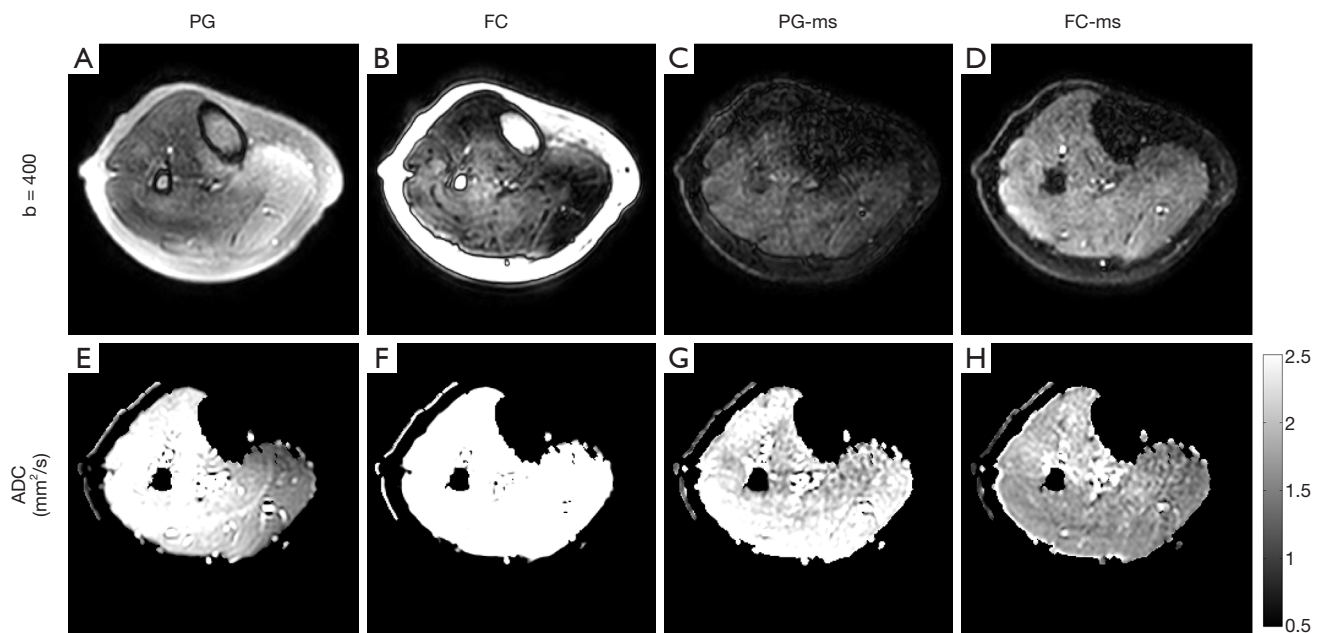


Figure 7 Typical single direction diffusion-weighted images of the calf muscle (A-D) and corresponding ADC maps (E-H). Four variations of the dprep-TSE sequence were used for the acquisition: pulsed gradient, without magnitude stabilizers (PG); pulsed gradient, with magnitude stabilizers (PG-ms); flow-compensation, without magnitude stabilizers (FC); flow-compensation, with magnitude stabilizers (FC-ms). Without magnitude stabilizers, DWIs show clear spatial magnitude variation (A,B) and ADC maps are overestimated (E,F). With magnitude stabilizers but without flow-compensation, severe artifacts can be observed in DWI due to phase inconsistency across shots (C). The resulted ADC map is therefore incorrect (G). The combination of flow-compensation and magnitude stabilizers gives artifact-free DWI (D) and reasonable ADC map (H).

inhomogeneity. Single-shot dprep-TSE has been shown to be successful in previous studies (23,26). Extending the dprep-TSE to a multi-shot acquisition in order to accommodate high-resolution requires a comprehensive understanding of not only the magnitude but also the phase of the signal in the presence of phase errors. We have shown analytically, through simulation, and experimentally that phase errors as a result of the diffusion preparation cause both magnitude and phase modulation of the acquired data. When the phase error is constant within a voxel and the T1 relaxation can be ignored, the resulted phase and magnitude modulation is rather simple: magnitude modulation with $|\cos\phi_{\text{voxel}}|$ and phase toggle between $\pi/2$ and $3\pi/2$ states.

T1 recovery during the time between the tip-up pulse and the excitation pulse of the TSE readout contaminates the prepared signal with freshly recovered magnetization. The ratio between the unprepared magnetization and prepared magnetization at the beginning of the TSE readout depends on the phase error, T1 relaxation effects, T2 relaxation effects, the diffusivity of the tissue, and the

diffusion encoding parameters (Figure 4A,B). This T1 recovery effect has two negative impacts on the dprep-TSE sequence. Firstly, the DW contrast is contaminated by the T1-weighted contrast, leading to incorrect quantification of diffusion parameters. Secondly, even when the phase error is unchanged from repetition to repetition, such as in the case of eddy-current-induced phase errors, the phase-error-induced magnitude modulation cannot be completely removed with the use of phase cycling and the combination of data based on the SOS method (Figures 5,6). Therefore, when motion-compensated diffusion encoding is used, the leftover eddy-current-induced phase errors have to be attended to for accurate quantification of diffusion parameters and phase cycling and SOS is not an appropriate method.

It is worth to note that while the motion-compensated diffusion encoding mitigates MiPe, it might induce more severe eddy current effects. Therefore, if the MiPe is not significant, employing motion-compensated diffusion encoding might do more harm than good and worsen the

magnitude modulation in acquisitions without magnitude stabilizers (*Figure 7A,B*).

When the phase error is uniform within a voxel (no intra-voxel dephasing), the magnitude modulation can be removed by using magnitude stabilizers at a cost of 50% signal loss [Eq. [16]]. The phase modulation, however, remains. In a multi-shot acquisition, if the phase error is unchanged from shot to shot, such as in the case of eddy-current-induced phase error, the phase-error-induced phase modulation is consistent across shots and can be ignored. If the phase error varies from shot to shot, which is the case for MiPe, the inconsistent signal phase modulation corrupts images when shots are combined (*Figure 7C*). When flow-compensated diffusion encoding is used, motion-induced phase inconsistency across shots is reduced yielding uncorrupted shot-combined images in the scanned calf muscle (*Figure 7D,H*). However, even with flow-compensation, images acquired without magnitude stabilizers (*Figure 7B*) still show significant magnitude modulation due to unresolved eddy-current-induced phase errors.

In addition to removing the phase-error-induced magnitude modulation, the employment of magnitude stabilizers eliminates the contamination of the diffusion prepared signal with the unprepared T1-recovered signal that arises due to the T1 relaxation during the time tm between the tip-up RF pulse and the TSE excitation. Although tm is most of the times significantly smaller than T1, it has been shown in our phantom experiment that this unprepared T1 recovered signal is not negligible in DW experiments when magnitude stabilizers are not used and can result in erroneous quantification of diffusion metrics.

Bright fat signal is a well-known problem in T2-weighted images acquired with TSE readout (37). When diffusion encoding is applied, the reduced signal of muscle due to diffusion-encoding attenuation makes the fat signal (which was suppressed by SPAIR) comparable to the muscle signal (*Figure 7A,B*). Without magnitude stabilizers, the combination of motion-, and eddy-current-induced magnitude modulation causes fluctuation in relative amplitude between fat and muscle. Depending on the difference of the phase errors between muscle region and fat region, it is possible that the residual, incompletely suppressed fat signal comes out equal or even higher than the water signal (*Figure 7A,B*). Further investigation is still needed but we observe that the presence of magnitude stabilizers results in images with better and more stable fat suppression (*Figure 7D*).

Conclusions

Through analytical derivation, simulations, and experimental data we have shown that in dprep-TSE sequences, phase uncertainty before the tip-up RF pulse leads to magnitude and phase modulation in the acquired TSE-signal. Sources of phase uncertainty were identified as motion and eddy currents. In many cases, MiPe can be minimized with motion-compensated diffusion encoding. However, the signal magnitude modulation due to eddy-current-induced phase errors remains, which might cause erroneous quantification of diffusion parameters. At a cost of 50% signal loss, magnitude stabilizers eliminate the phase-error-induced magnitude modulation regardless of its source, but maintain the dependence of the signal phase on phase errors. Therefore, a successful multi-shot dprep-TSE experiment requires further steps to minimize the phase inconsistency across shots.

For accurate and reproducible diffusion parameter estimation, we suggest that magnitude stabilizers are a must in dprep-TSE sequences, regardless of the diffusion-preparation module and the number of shots employed. When multi-shot is used, in addition to magnitude stabilizers, motion-compensated diffusion encoding and/or phase navigation is needed to guarantee phase consistency across shots for artifact-free DW images.

Acknowledgements

The present work was partly supported by Philips Healthcare.

Footnote

Conflicts of Interest: H Kooijmann is an employer of Philips Healthcare. DC Karampinos receives grant support from Philips Healthcare. AT Van and B Cervantes have no conflicts of interest to declare.

Ethical Statement: This study was approved by the local ethics committee (approval number: 5679/13).

References

1. Jezard P, Barnett AS, Pierpaoli C. Characterization of and correction for eddy current artifacts in echo planar diffusion imaging. *Magn Reson Med* 1998;39:801-12.
2. Reese TG, Heid O, Weisskoff RM, Wedeen VJ. Reduction

- of eddy-current-induced distortion in diffusion MRI using a twice-refocused spin echo. *Magn Reson Med* 2003;49:177-82.
3. Le Bihan D, Poupon C, Amadon A, Lethimonnier F. Artifacts and pitfalls in diffusion MRI. *J Magn Reson Imaging* 2006;24:478-88.
 4. Butts K, Pauly J, de Crespigny A, Moseley M. Isotropic diffusion-weighted and spiral-navigated interleaved EPI for routine imaging of acute stroke. *Magn Reson Med* 1997;38:741-9.
 5. Holdsworth SJ, Skare S, Newbould RD, Bammer R. Robust GRAPPA-accelerated diffusion-weighted readout-segmented (RS)-EPI. *Magn Reson Med* 2009;62:1629-40.
 6. Porter DA, Heidemann RM. High resolution diffusion-weighted imaging using readout-segmented echo-planar imaging, parallel imaging and a two-dimensional navigator-based reacquisition. *Magn Reson Med* 2009;62:468-75.
 7. Anderson AW, Gore JC. Analysis and correction of motion artifacts in diffusion weighted imaging. *Magn Reson Med* 1994;32:379-87.
 8. Liu C, Bammer R, Kim DH, Moseley ME. Self-navigated interleaved spiral (SNAILS): application to high-resolution diffusion tensor imaging. *Magn Reson Med* 2004;52:1388-96.
 9. O'Halloran R, Aksoy M, Aboussouan E, Peterson E, Van A, Bammer R. Real-time correction of rigid body motion-induced phase errors for diffusion-weighted steady-state free precession imaging. *Magn Reson Med* 2015;73:565-76.
 10. Ordidge RJ, Helpert JA, Qing ZX, Knight RA, Nagesh V. Correction of Motional Artifacts in Diffusion-Weighted Mr-Images Using Navigator Echoes. *Magnetic Resonance Imaging* 1994;12:455-60.
 11. Van AT, Hernando D, Sutton BP. Motion-induced phase error estimation and correction in 3D diffusion tensor imaging. *IEEE Trans Med Imaging* 2011;30:1933-40.
 12. Van AT, Karampinos DC, Georgiadis JG, Sutton BP. K-space and image-space combination for motion-induced phase-error correction in self-navigated multicoil multishot DWI. *IEEE Trans Med Imaging* 2009;28:1770-80.
 13. Beaulieu CF, Zhou X, Cofer GP, Johnson GA. Diffusion-weighted MR microscopy with fast spin-echo. *Magn Reson Med* 1993;30:201-6.
 14. Brockstedt S, Thomsen C, Wirestam R, Holtas S, Stahlberg F. Quantitative diffusion coefficient maps using fast spin-echo MRI. *Magn Reson Imaging* 1998;16:877-86.
 15. Oshio K, Feinberg DA. GRASE (Gradient- and spin-echo) imaging: a novel fast MRI technique. *Magn Reson Med* 1991;20:344-9.
 16. Schick F. SPLICE: sub-second diffusion-sensitive MR imaging using a modified fast spin-echo acquisition mode. *Magn Reson Med* 1997;38:638-44.
 17. Le Roux P. Non-CPMG Fast Spin Echo with full signal. *J Magn Reson* 2002;155:278-92.
 18. Poon CS, Henkelman RM. Practical T2 quantitation for clinical applications. *J Magn Reson Imaging* 1992;2:541-53.
 19. Pipe JG, Farthing VG, Forbes KP. Multishot diffusion-weighted FSE using PROPELLER MRI. *Magn Reson Med* 2002;47:42-52.
 20. Norris DG, Bornert P, Reese T, Leibfritz D. On the application of ultra-fast RARE experiments. *Magn Reson Med* 1992;27:142-64.
 21. Lee H, Price RR. Diffusion imaging with the MP-RAGE sequence. *J Magn Reson Imaging* 1994;4:837-42.
 22. Thomas DL, Pell GS, Lythgoe MF, Gadian DG, Ordidge RJ. A quantitative method for fast diffusion imaging using magnetization-prepared TurboFLASH. *Magn Reson Med* 1998;39:950-60.
 23. Alsop DC. Phase insensitive preparation of single-shot RARE: application to diffusion imaging in humans. *Magn Reson Med* 1997;38:527-33.
 24. Cervantes B, Weidlich D, Kooijman H, Rummeny EJ, Haase A, Kirschke JS, Karampinos DC. High-resolution DWI of the lumbar plexus using B1-insensitive velocity-compensated diffusion-prepared 3D TSE. *Proc Intl Soc Mag Reson Med* 2016;24:4474.
 25. Cervantes B, Zhang Q, van de Ven K, Kooijman H, Rummeny EJ, Haase A, Strijkers GJ, Kirschke JS, Nederveen AJ, Karampinos DC. High-resolution DTI of distal peripheral nerves using flow-compensated diffusion-prepared 3D TSE. *Proc Intl Soc Mag Reson Med* 2016;24:4530.
 26. Jeong EK, Kim SE, Kholmovski EG, Parker DL. High-resolution DTI of a localized volume using 3D single-shot diffusion-weighted STimulated echo-planar imaging (3D ss-DWSTEPI). *Magn Reson Med* 2006;56:1173-81.
 27. Jeong EK, Kim SE, Parker DL. High-resolution diffusion-weighted 3D MRI, using diffusion-weighted driven-equilibrium (DW-DE) and multishot segmented 3D-SSFP without navigator echoes. *Magn Reson Med* 2003;50:821-9.
 28. Nguyen C, Fan Z, Sharif B, He Y, Dharmakumar R, Berman DS, Li D. In vivo three-dimensional high resolution cardiac diffusion-weighted MRI: a motion compensated diffusion-prepared balanced steady-state free precession approach. *Magn Reson Med* 2014;72:1257-67.

29. Nguyen C, Fan Z, Xie Y, Pang J, Speier P, Bi X, Kobashigawa J, Li D. In vivo diffusion-tensor MRI of the human heart on a 3 tesla clinical scanner: An optimized second order (M2) motion compensated diffusion-preparation approach. *Magn Reson Med* 2016;76:1354-63.
30. Nolte UG, Finsterbusch J, Frahm J. Rapid isotropic diffusion mapping without susceptibility artifacts: whole brain studies using diffusion-weighted single-shot STEAM MR imaging. *Magn Reson Med* 2000;44:731-6.
31. Xie Y, Yu W, Fan Z, Nguyen C, Bi X, An J, Zhang T, Zhang Z, Li D. High resolution 3D diffusion cardiovascular magnetic resonance of carotid vessel wall to detect lipid core without contrast media. *J Cardiovasc Magn Reson* 2014;16:67.
32. Xie Y, Yu W, Fan Z, Nguyen CT, An J, Zhang Z, Li D. High resolution 3D diffusion MRI of carotid plaque on 3T. *J Cardiovasc Magn Reson* 2014;16:O28.
33. Zhang Q, Cervantes B, Karampinos DC, Coolen BF, Nederveen AJ, Strijkers GJ. High resolution 3D diffusion imaging of carotid vessel wall using stimulated echo based diffusion prepared turbo spin echo sequence. *Proc Intl Soc Mag Reson Med* 2016;24:959.
34. Cervantes B, Bauer JS, Zibold F, Kooijman H, Settles M, Haase A, Rummeny EJ, Wortler K, Karampinos DC. Imaging of the lumbar plexus: Optimized refocusing flip angle train design for 3D TSE. *J Magn Reson Imaging* 2016;43:789-99.
35. Parrish T, Hu X. A new T2 preparation technique for ultrafast gradient-echo sequence. *Magn Reson Med* 1994;32:652-7.
36. Mugler JP, 3rd. Optimized three-dimensional fast-spin-echo MRI. *J Magn Reson Imaging* 2014;39:745-67.
37. Henkelman RM, Hardy PA, Bishop JE, Poon CS, Plewes DB. Why fat is bright in RARE and fast spin-echo imaging. *J Magn Reson Imaging* 1992;2:533-40.

Cite this article as: Van AT, Cervantes B, Kooijman H, Karampinos DC. Analysis of phase error effects in multishot diffusion-prepared turbo spin echo imaging. *Quant Imaging Med Surg* 2017;7(2):238-250. doi:10.21037/qims.2017.04.01